Inorganic Chemistry

Article

Synthesis and Characterization of Tetrahedral and Square Planar Bis(iminopyrrolyl) Complexes of Cobalt(II)

Sónia A. Carabineiro,[†] Leonel C. Silva,[†] Pedro T. Gomes,*,[†] Laura C. J. Pereira,[‡] Luís F. Veiros,[†] Sofia I. Pascu,[§] M. Teresa Duarte,[†] Sónia Namorado,[†] and Rui T. Henriques[||]

Centro de Química Estrutural, Departamento de Engenharia Química e Biológica, Instituto Superior Técnico, Av. Rovisco Pais, 1049-001 Lisboa, Portugal, Departamento de Química, Instituto Tecnológico e Nuclear/CFMCUL, Estrada Nacional 10, 2686-953 Sacavém, Portugal, Chemistry Research Laboratory, University of Oxford, OX1 2TA Oxford, U.K., and Instituto de Telecomunicações, Instituto Superior Técnico, Av. Rovisco Pais, 1049-001 Lisboa, Portugal

Received November 8, 2006

A series of 2-iminopyrrole ligand precursors with increasing bulkiness [HNC$_4$H$_3$C(R)=N-2,6-R′$_2$C$_6$H$_3$] (R = R′ = H, **1a**; R = Me, R′= H, **1b**; R = H, R′ = Me, **1c**; R = R′ = Me, **1d**; R = H, R′ = ^{i}Pr, **1e**; R = Me, R′ = ^{i}Pr, **1f**) were synthesized and deprotonated with NaH to give the corresponding iminopyrrolyl sodium salts **2a**–**f**. A set of homoleptic bis-ligand Co(II) complexes of the type [Co(κ^2N,N′-NC$_4$H$_3$C(R)=N-2,6-R′$_2$C$_6$H$_3$)$_2$] (R = R′= H, **3a**; R = Me, R′= H, **3b**; R = H, R′ = Me, **3c**; R = R′ = Me, **3d**; R = H, R′ = ^{i}Pr, **3e**; R = Me, R′ = ^{i}Pr, **3f**) was prepared by reaction of CoCl$_2$ with the corresponding iminopyrrolyl sodium salts **2a**–**f**. The new complexes were characterized by elemental analysis, magnetic susceptibility measurements, in powder and in solution, UV/vis/NIR, and, in some cases, X-ray crystallography. According to X-ray diffraction and magnetic measurements, the Co complexes **3a**–**e** proved to be tetrahedral, which is the preferred geometry for Co(II) compounds. However, a square planar geometry is observed in the case of **3f**, as determined by several characterization techniques. In this case, DFT calculations suggest the square planar geometry is slightly more stable than the tetrahedral one probably due to a combination of steric and electronic reasons.

Introduction

The use of iminopyrrolyl ligands in the synthesis of transition-metal compounds is known, but the first rational synthetic reports on the subject were presented by Holm et al. in the 1960s, for compounds of the type [M(iminopyrrolyl)$_2$] (M(II) = Co, Ni, Pd, Cu, Zn).[1] For cobalt, due to the use of aerobic conditions, less bulky R groups gave rise to oxidized octahedral complexes of the type [Co^{III}(iminopyrrolyl)$_3$][2] (Chart 1, **A**), and only the use of *tert*-butyl as substituent of the imine group provided an efficient stoichiometric control and enabled the synthesis and characterization of the corresponding [Co^{II}(iminopyrrolyl)$_2$].[1,2] All

the characterization data for this compound, including the X-ray diffraction study,[3] have shown a tetrahedral structure around the Co atom (Chart 1, **B**). Very recently, the same type of geometry was found in a Co(II) dinuclear [4 + 4] helical complex of a diiminodipyrrolyl ligand containing also *tert*-butyl substituents.[4]

In recent times, α-diimine ligands with bulky aryl substituents gave rise to group 10 metal complexes which are very active α-olefin polymerization catalysts.[5,6] This boosted the search for new sterically tunable nitrogen-based polydentate ligands.[6–8] It is known that the stereochemical control of the metal centers provides efficient steric shielding of a

* To whom correspondence should be addressed. E-mail: pedro.t.gomes@ist.utl.pt. Phone: +351 218419612. Fax: +351 218419612.
† Instituto Superior Técnico (CQE).
‡ Instituto Tecnológico e Nuclear/CFMCUL.
§ University of Oxford.
|| Instituto Superior Técnico (IT).

(1) Holm, R. H.; Chakravorty, A.; Theriot, L. J. *Inorg. Chem.* **1966**, *5*, 625–635 and references cited therein.
(2) Chakravorty, A.; Holm, R. H. *Inorg. Chem.* **1964**, *3*, 1521–1524.
(3) Wei, C. H. *Inorg. Chem.* **1972**, *11*, 1100–1105.
(4) Reid, S. D.; Blake, A. J.; Wilson, C.; Love, J. B. *Inorg. Chem.* **2006**, *45*, 636–643.
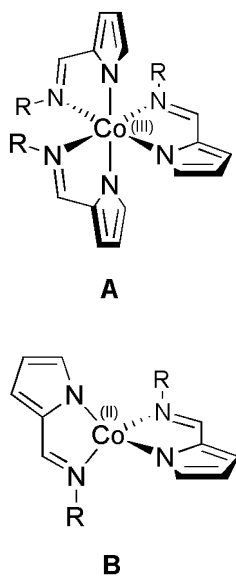(5) Johnson, L. K.; Killian, C. M.; Brookhart, M. *J. Am. Chem. Soc.* **1995**, *117*, 6414–6415.
(6) Ittel, S. D.; Johnson, L. K.; Brookhart, M. *Chem. Rev.* **2000**, 1169–1203.
(7) Britovsek, G. J. P.; Gibson, V. C.; Wass, D. F. *Angew. Chem., Int. Ed.* **1999**, *38*, 428–447.
(8) Gibson, V. C.; Spitzmesser, S. K. *Chem. Rev.* **2003**, *103*, 283–315.

Chart 1

A

B

large sector of the coordination sphere and kinetic stabilization, leading to modified reactivities and increased stability of the complexes. With this perspective in view, several mono- or bis(iminopyrrolyl) early-transition-metal complexes have been reported in the literature, in which the imine substituents were bulky aryl groups.[9] Gibson et al. reported bis(iminopyrrolyl) complexes of Cr(II) and Cr(III).[10,11] Bis-(iminopyrrolyl) complexes of group 4 metals were prepared by Mashima et al. (Zr−diamido complexes),[9,12] Bochmann et al. (Zr−dichloro and −diamido complexes),[13] Fujita et al. (Ti−dichloro complexes),[14−17] and Okuda et al. (Zr− and Hf−dibenzyl complexes).[18,19] Bis(iminopyrrolyl) chloro, amido, or alkyl complexes of rare earth metals have also been reported.[20,21]

Other authors have prepared homoleptic transition-metal complexes of the type [M(iminopyrrolyl)$_2$] (M = Co,[13] Ni,[13] Zn[22]), similar to those isolated by Holm et al. (see above)

but in which the imine substituent R is the sterically demanding 2,6-diisopropylphenyl group. The latter Co compound, which is the second known example of a mononuclear Co(II) bis(iminopyrrolyl) complex reported so far, was only characterized by elemental analysis and mass spectrometry, but no other information about its molecular structure was reported.[13]

It is known that tetracoordinated Co(II) compounds containing bidentate nitrogen-based chelating ligands show a clear preference for high-spin tetrahedral geometries ($S = 3/2$).[23,24] The majority of low-spin Co(II) ($S = 1/2$) complexes are square planar chelates of tetradentate macrocycles, such as porphyrins or Schiff bases derivatives, which, due to their intrinsic structural features, impose this type of geometry around the metal center.[25] However, there are a few cases of N,O[26−28] or S,S[29−31] bidentate chelating ligands which give rise to square planar Co(II) complexes or compounds which exhibit tetrahedral−square planar equilibria.

An example of the geometry and magnetic properties tuning of a Co(II) center is that imposed by the geometric constraints of a macrocycle ligand, as reported by Lippard et al.[32] In this work, where a series of Co(II) complexes of tropocoronand macrocycles was synthesized, it was shown that as the macrocycle is expanded by the introduction of an increasing number of methylene groups, the geometry around the Co(II) center switches abruptly from square planar ($S = 1/2$) to tetrahedral geometry ($S = 3/2$). These geometrical changes may cause different reactivity patterns toward the activation of small molecules.[25,32]

We have been interested in the chemistry of bulky iminopyrrolyl ligands and their role in ethylene oligo/polymerization catalysis when coordinated to late transition metals.[33] Here we describe the synthesis and characterization of a series of [Co^{II}(iminopyrrolyl)$_2$] complexes in which the bidentate chelating ligands encompass increasing bulkiness. The ligands used derive either from known formiminopyrroles with variable size aryl substituents of the imine nitrogen (Ph, 2,6-Me$_2$Ph and 2,6-^{i}Pr$_2$Ph) or from new acetiminopyrroles, synthesized as described below (Scheme 1). This study aims to determine whether the Co(II) coordination sphere

(9) Mashima, K.; Tsurugi, H. *J. Organomet. Chem.* **2005**, *690*, 4414−4423.
(10) Gibson, V. C.; Maddox, P. J.; Newton, C.; Redshaw, C.; Solan, G. A.; White, A. J. P.; Williams, D. J. *Chem. Commun*. **1998**, 1651−1652.
(11) Gibson, V. C.; Newton, C.; Redshaw, C.; Solan, G. A.; White, A. J. P.; Williams, D. J. *J. Chem. Soc., Dalton Trans.* **2002**, 4017−4023.
(12) Matsuo, Y.; Mashima, K.; Tani, K. *Chem. Lett.* **2000**, 1114−1115.
(13) Dawson, D. M.; Walker, D. A.; Thornton-Pett, M.; Bochman, M. *J. Chem. Soc., Dalton Trans.* **2000**, 459−466.
(14) Yoshida, Y.; Matsiu, S.; Takagi, Y.; Mitani, M.; Nitabaru, M.; Nakano, T.; Tanaka, H.; Fujita, T. *Chem. Lett.* **2000**, 1270−1271.
(15) Yoshida, Y.; Matsiu, S.; Takagi, Y.; Mitani, M.; Nakano, T.; Tanaka, H.; Kashiwa, N.; Fujita, T. *Organometallics* **2001**, *20*, 4793−4799.
(16) Yoshida, Y.; Saito, J.; Mitani, M.; Takagi, Y.; Matsui, S.; Ishii, S.; Nakano, T.; Kashiwa, N.; Fujita, T. *Chem. Commun.* **2002**, 1298−1299.
(17) Yoshida, Y.; Mohri, J.; Ishii, S.; Mitani, M.; Saito, J.; Matsui, S.; Makio, H.; Nakano, T.; Tanaka, H.; Onda, M.; Yamamoto, Y.; Mizuno, A.; Fujita, T. *J. Am. Chem. Soc.* **2004**, *126*, 12023−12032.
(18) Matsui, S.; Spaniol, T. P.; Tagaki, Y.; Yoshida, Y.; Okuda, J. *J. Chem. Soc., Dalton Trans.* **2002**, 4529−4531.
(19) Matsui, S.; Yoshida, Y.; Tagaki, Y.; Spaniol, T. P.; Okuda, J. *J. Organomet. Chem.* **2004**, *689*, 1155−1164.
(20) Matsuo, Y.; Mashima, K.; Tani, K. *Organometallics* **2001**, *20*, 3510−3518.
(21) Cui, C.; Shafir, A.; Reeder, C. L.; Arnold, J. *Organometallics* **2003**, *22*, 3357−3359.

(22) Hao, H.; Bhandari, S.; Ding, Y.; Roesky, H. W.; Magull, J.; Schmidt, H. G.; Noltemeyer, M.; Cui, C. *Eur. J. Inorg. Chem.* **2002**, 1060−1065.
(23) Everett, G. W., Jr.; Holm, R. H. *J. Am. Chem. Soc.* **1966**, *88*, 2442−2451.
(24) Everett, G. W., Jr.; Holm, R. H. *Inorg. Chem.* **1968**, *7*, 776−785.
(25) Jones, R. D.; Summerville, D. A.; Basolo, F. *Chem. Rev.* **1979**, *79*, 139−179.
(26) Rudolf, M. F.; Wolny, J.; Ciunik, Z.; Chmielewski, P. *J. Chem. Soc., Chem. Commun.* **1988**, 1006−1007.
(27) Wolny, J. A.; Rudolf, M. F.; Ciunik, Z.; Gatner, K.; Wolowiec, S. *J. Chem. Soc., Dalton Trans.* **1993**, 1611−1622.
(28) Manhas, B. S.; Verma, B. C.; Kalia, S. B. *Polyhedron* **1995**, *14*, 3549−3556.
(29) Maki, A. H.; Edelstein, N.; Davison, A.; Holm, R. H. *J. Am. Chem. Soc.* **1964**, *86*, 4580−4587.
(30) Fitzgerald, R. J.; Brubaker, G. R. *Inorg. Chem.* **1969**, *8*, 2265−2267.
(31) Gregson, A. K.; Martin, R. L.; Mitra, S. *Chem. Phys. Lett.* **1970**, *5*, 310−311.
(32) Jaynes, B. S.; Doerrer, L. H.; Liu, S.; Lippard, S. J. *Inorg. Chem.* **1995**, *34*, 5735−5744.
(33) Bellabarba, R. M.; Gomes, P. T.; Pascu, S. I. *Dalton Trans.* **2003**, 4431−4436.

Scheme 1. Synthesis of Ligand Precursors **1a−f**

1a R = R'= H, **1d** R = R' = Me
1b R = Me, R'= H **1e** R = H, R' = ^{i}Pr
1c R = H, R' = Me **1f** R = Me, R' = ^{i}Pr
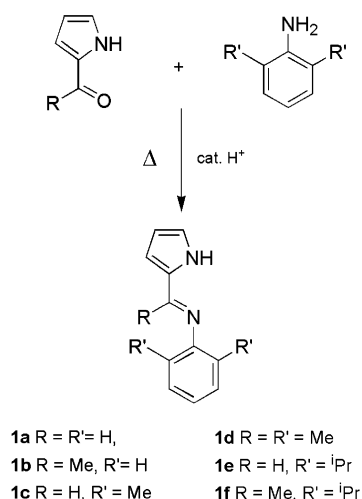
can be tuned from tetrahedral to the rarely observed square planar geometry using this type of bis-chelating ligand. For this purpose, structural and spectroscopic investigations have been carried out on the compounds synthesized, such as single-crystal X-ray diffraction, magnetic susceptibility measurements in solid and in solution, UV/vis/NIR spectroscopy, and DFT calculations.

Experimental Section

General Considerations. All experiments dealing with air- and/ or moisture-sensitive materials were carried out under inert atmosphere using a dual vacuum/nitrogen line and standard Schlenk techniques. Nitrogen gas was supplied in cylinders by specialized companies (e.g., Air Liquide, etc.) and purified by passage through 4 Å molecular sieves. Unless otherwise stated, all reagents were purchased from commercial suppliers (e.g., Acros, Aldrich, Fluka) and used without further purification. All solvents to be used under inert atmosphere were thoroughly deoxygenated and dehydrated before use. They were dried and purified by refluxing over a suitable drying agent followed by distillation under nitrogen. The following drying agents were used: sodium (for toluene, diethyl ether, and tetrahydrofuran); calcium hydride (for hexane and dichloromethane). Deuterated solvents were dried by storage over 4 Å molecular sieves and degassed by the freeze−pump−thaw method. Solvents and solutions were transferred using a positive pressure of nitrogen through stainless steel cannulas, and mixtures were filtered in a similar way using modified cannulas that could be fitted with glass fiber filter disks.

Nuclear magnetic resonance (NMR) spectra were recorded on a Varian Unity 300 MHz spectrometer at the following frequencies: ^{1}H at 299.995 MHz; ^{13}C at 75.4296 MHz. Spectra were referenced internally using the residual protio solvent resonance relative to tetramethylsilane ($\delta = 0$). All chemical shifts are quoted in δ (ppm), and coupling constants are given in Hz. Multiplicities were abbreviated as follows: broad (br); singlet (s); doublet (d); triplet (t); quartet (q); heptet (h); multiplet (m). For air- and/or moisture-stable compounds, samples were dissolved in CDCl$_3$ and prepared in common NMR tubes. The NMR assignments of the pyrrole ring were made according to the X-ray labeling (see ligand precursor syntheses below). For air- and/or moisture-sensitive materials, samples were prepared in J. Young tubes, using a glovebox. Elemental analyses were obtained from the IST or ITN elemental analysis services.

Electronic spectra were recorded in a Perkin-Elmer Lambda 9 UV/vis/NIR spectrophotometer, between 200 and 1500 nm, at room temperature. Solution samples were prepared in a glovebox, by dissolving the complexes (or the ligand precursors) in freshly distilled toluene, to give rigorous solutions (in most cases 10^{-3} and 10^{-5} mol L^{-1}), and the corresponding spectra were obtained in quartz cells with optical lengths of 1 cm, under inert atmosphere. For comparison, solid-state samples were also measured in Nujol mulls, which were deposited on the inner surfaces of quartz cells. In the spectra obtained in solution, molar extinction coefficients (ϵ) were calculated for each absorption maximum.

Syntheses of 2-Formiminopyrrole Ligand Precursors (1a,c,e). A similar procedure used in a previous publication of our group (where mesitylaniline was employed)[33] was followed. This general procedure was adapted from the literature for **1a**[34,35] and **1e**:[13,36,37] 2-Formylpyrrole (10.0 mmol), the appropriate aniline (10 mmol), and a catalytic amount of *p*-toluenesulfonic acid were suspended in absolute ethanol (5 mL) in a 50 mL round-bottom flask fitted with a condenser and a CaCl$_2$ guard tube. The mixture was heated to reflux for 3 days (over the weekend). NaHCO$_3$ was added (while still hot) to neutralize the acid. The mixture was allowed to cool, CH$_2$Cl$_2$ was added, and the suspension was filtered through Celite and washed through with more CH$_2$Cl$_2$. After removal of all volatiles (in the rotary evaporator), the product was dissolved in refluxing hexane. A dark brown oil was decanted from the supernatant orange solution, which was stored at −20 °C to yield 1.04 g (61%) of a dark yellow microcrystalline solid of **1a**, 1.27 g (64%) of yellow-orange crystals of **1c**, or 1.62 g (70%) of orange-reddish crystals of **1e**.

Data for 1a. Anal. Found (calcd): C, 77.38 (77.62); H, 6.49 (5.92); N, 16.27 (16.46). NMR [δ_H (CDCl$_3$)]: 9.71 (1H, br s, pyrrole N*H*), 8.25 (1H, s, N=C*H*), 7.37 (2H, m, aryl *o*-H), 7.23−7.16 (3H, m, aryl *m*- and *p*-H), 6.83 (1H, m, pyrrole H3), 6.68 (1H, m, pyrrole H1), 6.27 (1H, m, pyrrole H2). NMR [δ_C (CDCl$_3$)]: 151.7 (aryl *ipso*-C), 150.0 (N=*C*H), 130.7 (pyrrole C4), 129.2 (aryl *m*-C), 125.5 (aryl *p*-C), 123.4 (pyrrole C1), 120.9 (aryl *o*-C), 116.8 (pyrrole C3), 110.4 (pyrrole C2).

Data for 1c. Anal. Found (calcd): C, 78.68 (78.75); H, 7.37 (7.12); N, 13.97 (14.13). NMR [δ_H (CDCl$_3$)]: 10.43 (1H, br, pyrrole N*H*), 7.95 (1H, s, N=C*H*), 7.06 (2H, d, J_{HH} = 7.5 Hz, aryl *m*-H), 6.95 (1H, t, J_{HH} = 7.5 Hz, aryl *p*-H), 6.59 (1H, m, pyrrole H3), 6.55 (1H, m, pyrrole H1), 6.21 (1H, m, pyrrole H2), 2.14 (6H, s, aryl *o*-C*H*$_3$). NMR [δ_C (CDCl$_3$)]: 153.2 (N=*C*H), 150.7 (aryl *ipso*-C), 130.0 (pyrrole C4), 128.3 (aryl *o*-C), 128.1 (aryl *m*-C), 123.9 (aryl *p*-C), 123.4 (pyrrole C1), 116.8−116.7 (pyrrole C3 and C1), 109.9 (pyrrole C2), 18.4 (aryl *o*-CH$_3$).

Data for 1e. Anal. Found (calcd): C, 80.50 (80.27); H, 8.41 (8.72); N, 10.35 (11.01). NMR [δ_H (CDCl$_3$)]: 10.97 (1H, br, pyrrole N*H*), 7.97 (1H, s, N=C*H*), 7.23−7.15 (3H, m, aryl *m*- and *p*-H), 6.60 (1H, m, pyrrole H1), 6.20 (1H, m, pyrrole H3), 6.15 (1H, m, pyrrole H2), 3.10 (2H, h, J_{HH} = 6.6 Hz, C*H*(CH$_3$)$_2$), 1.12 (12H, d, J_{HH} = 6.6 Hz, CH(C*H*$_3$)$_2$). NMR [δ_C (CDCl$_3$)]: 152.7 (N=*C*H), 148.5 (aryl *ipso*-C), 138.9 (aryl *o*-C), 129.9 (pyrrole C4), 124.5 (aryl *p*-C), 124.1 (pyrrole C1), 123.2 (aryl *m*-C), 116.6 (pyrrole C3), 109.9 (pyrrole C2), 27.9 (*C*H(CH$_3$)$_2$), 23.6 (CH(*C*H$_3$)$_2$).

Syntheses of 2-Acetiminopyrrole Ligand Precursors (1b,d,f). A similar procedure used in a previous publication of our group (where mesitylaniline employed)[33] was followed: 2-Acetylpyrrole

(34) Yeh, K.-N.; Barker, R. H. *Inorg. Chem.* **1967**, *6*, 830−833.
(35) Yoshida, Y.; Matsui, S.; Takagi, Y.; Mitani, M.; Nakano, T.; Tanaka, H.; Kashiwa, N.; Fujita, T. *Organometallics* **2001**, *20*, 4793−4799.
(36) Li, Y.-S.; Li, Y.-R.; Li, X.-F. *J. Organomet. Chem.* **2003**, *667*, 185−191.

(10.0 mmol) and the appropriate aniline (10 mmol) were placed in a 50 mL round-bottom flask with a catalytic amount of *p*-toluenesulfonic acid, under nitrogen. A CaCl$_2$ guard tube was fitted on top of the flask, and the whole flask was immersed in an oil bath and heated to 80 °C (**1b**), 120 °C (**1d**), or 140 °C (**1f**), for 5 days. To neutralize the acid, NaHCO$_3$ (powder) was added under nitrogen flow and while the mixture was still hot. The mixture was allowed to cool, and the remaining aniline was eliminated by trap-to-trap distillation. The resulting iminopyrrole compound was vacuum sublimed at ≈80 °C (10^{-2} mbar), further redissolved in boiling hexane, and filtered. The product was stored at −20 °C to yield 0.56 g (30%) of a dark yellow microcrystalline solid of **1b**, 0.47 g (22%) of a dark yellow microcrystalline powder of **1d**, or 0.43 g (16%) of bright yellow crystals of **1f**. In the case of the latter compound, crystals suitable for X-ray diffraction were obtained.

Data for 1b. Anal. Found (calcd): C, 78.28 (78.23); H, 6.40 (6.56); N, 15.36 (15.20). NMR [δ_H (CDCl$_3$)]: 9.55 (1H, br, pyrrole N*H*), 7.31 (2H, t, J_{HH} = 7.5 Hz, aryl *m*-H), 7.06 (1H, t, J_{HH} = 7.5 Hz, aryl *p*-H), 6.89 (1H, m, pyrrole H1), 6.78 (2H, d, J_{HH} = 7.5 Hz, aryl *o*-H), 6.65 (1H, m, pyrrole H3), 6.25 (1H, m, pyrrole H2), 2.11 (3H, s, N=C(C*H*$_3$)). NMR [δ_C (CDCl$_3$)]: 157.6 (N=*C*), 150.8 (aryl *ipso*-C), 132.5 (pyrrole C4), 128.9 (aryl *m*-C), 123.3 (aryl *p*-C), 121.8 (pyrrole C1), 120.4 (aryl *o*-C), 112.3 (pyrrole C3), 109.7 (pyrrole C2), 16.4 (N=C(*C*H$_3$)).

Data for 1d. Anal. Found (calcd): C, 78.93 (79.21); H, 7.51 (7.60); N, 12.99 (13.20). NMR [δ_H (CDCl$_3$)]: 10.01 (1H, br, pyrrole N*H*), 7.06 (2H, d, J_{HH} = 7.5 Hz, aryl *m*-H), 6.93 (1H, t, J_{HH} = 7.5 Hz, aryl *p*-H), 6.75−6.6 (2H, m, pyrrole H1 and H3), 6.22 (1H, m, pyrrole H2), 2.03 (6H, s, aryl *o*-C*H*$_3$), 1.95 (3H, s, N=C(C*H*$_3$)). NMR [δ_C (CDCl$_3$)]: 157.7 (N=*C*), 148.2 (aryl *ipso*-C), 132.0 (pyrrole C4), 127.8 (aryl *m*-C), 127.0 (aryl *o*-C), 122.9 (pyrrole C1), 121.9 (aryl *p*-C), 112.0 (pyrrole C3), 109.5 (pyrrole C2), 18.0 (aryl *o*-CH$_3$), 16.7 (N=C(*C*H$_3$)).

Data for 1f. Anal. Found (calcd): C, 80.60 (80.55); H, 10.58 (9.01); N, 10.33 (10.44). NMR [δ_H (CDCl$_3$)]: 9.72 (1H, br, pyrrole N*H*), 7.15−7.04 (3H, m, aryl *m*- and *p*-H), 6.69 (1H, m, pyrrole H1), 6.64 (1H, m, pyrrole H3), 6.24 (1H, m, pyrrole H2), 2.80 (2H, h, J_{HH} = 6.6 Hz, C*H*(CH$_3$)$_2$), 1.97 (3H, s, N=C(C*H*$_3$)), 1.11 (6H, d, J_{HH} = 6.6 Hz, CH(C*H*$_3$)(CH$_3$)), 1.08 (6H, d, J_{HH} = 6.6 Hz, CH(CH$_3$)(C*H*$_3$)). NMR [δ_C (CDCl$_3$)]: 157.5 (N=*C*H), 145.7 (aryl *ipso*-C), 137.3 (aryl *o*-C), 132.2 (pyrrole C4), 123.5 (aryl *p*-C), 123.0 (aryl *m*-C), 121.7 (pyrrole C1), 111.7 (pyrrole C3), 109.6 (pyrrole C2), 28.1 (*C*H(CH$_3$)$_2$), 23.3 (CH(*C*H$_3$)(CH$_3$)), 23.1 (CH(CH$_3$)-(*C*H$_3$)), 17.2 (N=C(*C*H$_3$)).

In Situ Synthesis of the Sodium Salts of Compounds 1a−f (2a−f). The same procedure followed in a previous publication of the group was used:[33] In a typical experiment, NaH (47.8 mg, 2 mmol) was suspended in tetrahydrofuran and 2 mmol of a neutral ligand precursor (**1a−f**) was slowly added as a solid under a counterflow of nitrogen. An immediate evolution of hydrogen occurred, and after some minutes, a solution of the sodium ligand salt was obtained and stirred for 90 min.

Synthesis of [Co(κ^{2}N,N′-NC$_4$H$_3$C(H)=NC$_6$H$_5$)$_2$] (3a). Anhydrous CoCl$_2$ (129.9 mg, 1 mmol) was suspended in tetrahydrofuran and cooled to −78 °C. The ligand sodium salt **2a** (186.3 mg, 2 mmol) was filtered and directly added dropwise to the CoCl$_2$ suspension, which was then stirred for 1 h. The mixture was allowed to warm to room temperature and further stirred for another 2 h.

Table 1. Crystal and Structure Refinement Data for Compounds **1f** and **3e,f**

param	**1f**	**3e**	**3f**
formula	C$_{18}$H$_{24}$N$_2$	C$_{34}$H$_{42}$CoN$_4$	C$_{36}$H$_{46}$CoN$_4$
M	268.40	565.65	593.72
λ/Å	0.710 73	0.710 69	0.681 40
T/K	180	100	150
cryst system	triclinic	triclinic	triclinic
space group	P$\bar{1}$	P$\bar{1}$	P$\bar{1}$
a/Å	8.7397(2)	10.952(3)	8.1966(14)
b/Å	11.5140(2)	16.279(5)	9.0582(16)
c/Å	17.0729(4)	18.283(4)	11.615(2)
α/deg	84.1779(8)	84.472(9)	69.060(2)
β/deg	77.7817(9)	80.667(10)	79.503(2)
γ/deg	71.7589(15)	80.271(8)	80.932(2)
V/Å^3	1593.59(6)	3162.3(14)	787.9(2)
Z	4	2	1
ρ_{calc}/g cm^{-3}	1.119	1.188	1.251
μ/mm^{-1}	0.066	0.570	0.575
θ_{max}/deg	27	19.90	32
tot. data	13 198	15 647	9484
unique data	7275	5439	5023
R$_{int}$	0.023	0.1347	0.023
R [$I > 3\sigma(I)$]	*0.0503*	*0.0770*	*0.0393*
wR	0.0635	0.1713	0.0419
goodness of fit	1.0091	0.906	1.1132
ρ_{min}, ρ_{max}	−0.28	−0.596	−0.33
	0.35	0.450	0.42

All volatiles were evaporated in vacuum, and the residue was extracted with hexane until extracts were colorless. The resulting orange-brown solution was concentrated and cooled to −20 °C to yield 0.32 g (80%) of a dark brown powder. Anal. Found (calcd): C, 66.45 (66.50); H, 4.83 (4.57); N, 14.05 (14.10).

Synthesis of [Co(κ^{2}N,N′-NC$_4$H$_3$C(Me)=NC$_6$H$_5$)$_2$] (3b). The same procedure described for **3a** was followed, but ligand sodium salt **2b** (184.2 mg, 2 mmol) was employed, to give 0.34 g (81%) of a brownish powder. Anal. Found (calcd): C, 67.56 (67.76); H, 5.75 (5.21); N, 13.14 (13.17).

Synthesis [Co(κ^{2}N,N′-NC$_4$H$_3$C(H)=N-2,6-Me$_2$C$_6$H$_3$)$_2$] (3c). The same procedure described for **3a** was followed, but ligand sodium salt **2c** (242.4 mg, 2 mmol) was employed, yielding 0.36 g (82%) of a red brown powder. Anal. Found (calcd): C, 68.72 (68.87); H, 6.21 (5.78); N, 11.98 (12.36).

Synthesis of [Co(κ^{2}N,N′-NC$_4$H$_3$C(Me)=N-2,6-Me$_2$C$_6$H$_3$)$_2$] (3d). The same procedure described for **3a** was followed, but ligand sodium salt **2d** (424.6 mg, 2 mmol) was employed, yielding 0.42 g (87%) of dark red small crystals. Anal. Found (calcd): C, 69.57 (69.84); H, 6.03 (6.28); N, 11.27 (11.64).

Synthesis of [Co(κ^{2}N,N′-NC$_4$H$_3$C(H)=N-2,6-^{i}Pr$_2$C$_6$H$_3$)$_2$] (3e). The same procedure described for **3a** was followed, but ligand sodium salt **2e** (506 mg, 2 mmol) was employed, yielding 0.46 g (82%) of dark red crystals. Crystals suitable for X-ray diffraction were obtained. Anal. Found (calcd): C, 71.94 (72.19); H, 7.72 (7.48); N, 9.65 (9.90).

Synthesis of [Co(κ^{2}N,N′-NC$_4$H$_3$C(Me)=N-2,6-^{i}Pr$_2$C$_6$H$_3$)$_2$] (3f). The same procedure described for **3a** was followed, but ligand sodium salt **2f** (536.8 mg, 2 mmol) was employed, yielding 0.54 g (91%) of bright red crystals. Crystals suitable for X-ray diffraction were obtained. Anal. Found (calcd): C, 73.02 (72.83); H, 8.10 (7.81); N, 9.12 (9.44).

X-ray Experimental Data. Crystallographic and experimental details of crystal structure determinations are given in Table 1. Crystals of compounds **1f** and **3e,f** were selected under an inert atmosphere, covered with polyfluoroether oil, and mounted on a nylon loop. Ligand precursor **1f** yielded weakly diffracting crystals. Data was collected at 180 K on a Nonius KappaCCD with graphite-

(37) Iverson, C. N.; Carter, C. A. S. G.; Baker, R. T.; Scollard, J. D.; Labinger, J. A.; Bercaw, J. E. *J. Am. Chem. Soc.* **2003**, *125*, 12674−12675.

monochromated Mo Kα radiation. Images were processed with DENZO and SCALEPACK programs.[38] Since crystals of **3f** were extremely small and weakly diffracting, synchrotron radiation was used to collect diffraction data on this compound. Data was collected at Station 9.8, Daresbury SRS, Warrington, Cheshire, U.K., using a Bruker SMART CCD diffractometer at 150K. For both **1f** and **3f**, structures were solved by direct methods using the program SIR92,[39] and refinements (on *F*) and graphical calculations were performed using the CRYSTALS[40] program suite.

For both **1f** and **3f** the non-hydrogen atoms were refined with anisotropic displacement parameters. Hydrogen atoms were located in Fourier maps and their positions adjusted geometrically (after each cycle of refinement) with isotropic thermal parameters. Chebychev weighting schemes and empirical absorption corrections were applied in each case.[41]

Crystallographic data for complex **3e** was collected using graphite-monochromated Mo Kα radiation ($\lambda = 0.710\,69$ Å) on a Bruker AXS-KAPPA APEX II diffractometer equipped with an Oxford Cryosystems open-flow nitrogen cryostat, at 150 K. Cell parameters were retrieved using Bruker[42] software and refined using Bruker SAINT[43] on all observed reflections. Absorption corrections were applied using SADABS.[44] Structure solution and refinement were performed using direct methods with the programs SIR97[45] and SHELXL[46] both included in the package of programs WINGX-version 1.70.01.[47] The poor diffracting power ($\theta_{max} = 20°$), size, and crystal quality ($R_{int} = 0.1347$) prevented the anisotropic refinement of all the non-hydrogen atoms; only Co atoms were refined with anisotropic displacement parameters. Due to the presence of two independent molecules in the asymmetric unit, the anisotropic refinement of the two molecules would lead to a very poor ratio of refined parameters/number of reflections that could prevent a good final and reliable refinement. All hydrogen atoms were inserted in idealized positions and allowed to refine riding in the parent carbon atom.

Figures were generated using ORTEP3.[48] Data was deposited in CCDC under the deposit nos. 624571 for **1f**, 624572 for **3e**, and 624573 for **3f**.

Magnetic Measurements. Magnetic susceptibility measurements in solution were carried out by the Evans method,[49,50] using a 3% solution of hexamethyldisiloxane in deuterated toluene as reference.

Magnetic measurements by the dc extraction method were performed on polycrystalline samples (10−20 mg) using a multi-purpose characterization system, MagLab 2000 (Oxford Instruments). The temperature dependence of the magnetic susceptibility was measured under magnetic fields of 5 T in the temperature range 1.7−300 K. The isothermal magnetization measurements up to 5 T and taken at different temperatures (1.7, 10, and 25 K) were also performed. The diamagnetism correction for the experimental data was estimated using the Pascal constants.[51]

Computational Details. All calculations were performed using the Gaussian 98 software package[52] and the B3LYP hybrid functional. That functional includes a mixture of Hartree−Fock[53] exchange with DFT[54] exchange correlation, given by Becke's three parameter functional[55] with the Lee, Yang, and Parr correlation functional, which includes both local and nonlocal terms.[56,57] The geometry optimizations were accomplished without symmetry constraints using a LanL2DZ basis set[58] for all atoms (B1). Single point energy calculations were performed on the B3LYP/B1 geometries, using the same functional and a standard 6-311G(d,p) basis set[59] (B2) for all elements. Spin contamination was carefully monitored for all calculations. The values of $\langle S^2 \rangle$ indicate minor spin contamination and are presented in the Supporting Information.

Given the known dependence of relative spin-state energies on the amount of exact exchange included in the functional,[60−62] energy calculations were repeated with a modified B3LYP functional (B3LYP*) with only 15% exact (Hartree−Fock) exchange and, also, with BP86, a "pure" DFT functional.[63] Low-spin species are increasingly favored with the amount of the exact exchange included in the functional, as expected,[60] but the general trend is maintained. The energy values discussed in the text (B3LYP/B2//B3LYP/B1) are the ones that fit better the experimental results.

(38) Otwinowski, Z.; Minor, W. In *Methods in Enzymology*; Carter, C. N., Jr., Sweet, R. M., Eds.; Academic Press: New York, 1996; p 276.
(39) SIR92: Altomare, A.; Cascarano, G. L.; Giacovazzo, C.; Guagliardi, A. *J. Appl. Crystallogr.* **1993**, *26*, 343−350.
(40) (a) Watkin, D. J.; Prout, C. K.; Carruthers, J. R.; Betteridge, P. W. *CRYSTALS*; Oxford University: Oxford, U.K., 1996. (b) Betteridge, P. W.; Carruthers, J. R.; Cooper, R. I.; Prout, K.; Watkin, D. J. *J. Appl. Crystallogr.* **2003**, *36*, 1487. (c) Watkin, D. J.; Prout, C. K.; Pearce, L. J. *CAMERON*; Oxford University: Oxford, U.K., 1996.
(41) Walker, N.; Stuart, D. *Acta Crystallogr., Sect. A* **1983**, *39*, 158−166.
(42) *SMART Software for the CCD detector System*, version 5.625; Bruker AXS Inc.: Madison, WI, 2001.
(43) *SAINT Software for the CCD detector System*, version 7.03; Bruker AXS Inc.: Madison, WI, 2004.
(44) Sheldrick, G. M. *SADABS*, version 2.10; Bruker AXS Inc.: Madison, WI, 2003.
(45) SIR97: Altomare, A.; Burla, M. C.; Camalli, M.; Cascarano, G. L.; Giacovazzo, C.; Guagliardi, A.; Moliterni, A. G. G.; Polidori, G.; Spagna, R. *J. Appl. Crystallogr.* **1999**, *32*, 115−119.
(46) Sheldrick, G. M. *SHELX97-Programs for Crystal Structure Analysis*, release 97-2; Institüt für Anorganische Chemie der Universität: Tammanstrasse 4, D-3400 Göttingen, Germany, 1998.
(47) Farrugia, L. J. *J. Appl. Crystallogr.* **1999**, *32*, 837−838.
(48) ORTEP3 for Windows: Farrugia, L. J. *J. Appl. Crystallogr.* **1997**, *30*, 565.
(49) Evans, D. F. *J. Chem. Soc.* **1959**, 2003−2005.
(50) Sur, S. K. *J. Magn. Res.* **1989**, *82*, 169−173.
(51) Carlin, R. L. In *Magnetochemistry*; Springer-Verlag: Berlin, 1986.
(52) Frisch, M. J.; Trucks, G. W.; Schlegel, H. B.; Scuseria, G. E.; Robb, M. A.; Cheeseman, J. R.; Zakrzewski, V. G.; Montgomery, J. A., Jr.; Stratmann, R. E.; Burant, J. C.; Dapprich, S.; Millam, J. M.; Daniels, A. D.; Kudin, K. N.; Strain, M. C.; Farkas, O.; Tomasi, J.; Barone, V.; Cossi, M.; Cammi, R.; Mennucci, B.; Pomelli, C.; Adamo, C.; Clifford, S.; Ochterski, J.; Petersson, G. A.; Ayala, P. Y.; Cui, Q.; Morokuma, K.; Malick, D. K.; Rabuck, A. D.; Raghavachari, K.; Foresman, J. B.; Cioslowski, J.; Ortiz, J. V.; Stefanov, B. B.; Liu, G.; Liashenko, A.; Piskorz, P.; Komaromi, I.; Gomperts, R.; Martin, R. L.; Fox, D. J.; Keith, T.; Al-Laham, M. A.; Peng, C. Y.; Nanayakkara, A.; Gonzalez, C.; Challacombe, M.; Gill, P. M. W.; Johnson, B. G.; Chen, W.; Wong, M. W.; Andres, J. L.; Head-Gordon, M.; Replogle, E. S.; Pople, J. A. *Gaussian 98*, revision A.7; Gaussian, Inc.: Pittsburgh, PA, 1998.
(53) Hehre, W. J.; Radom, L.; Schleyer, P. v. R.; Pople, J. A. *Ab Initio Molecular Orbital Theory*; John Wiley & Sons: New York, 1986.
(54) Parr, R. G.; Yang, W. *Density Functional Theory of Atoms and Molecules*; Oxford University Press: New York, 1989.
(55) Becke, A. D. *J. Chem. Phys.* **1993**, *98*, 5648−5652.
(56) Miehlich, B.; Savin, A.; Stoll, H.; Preuss, H. *Chem. Phys. Lett.* **1989**, *157*, 200−206.
(57) Lee, C.; Yang, W.; Parr, G. *Phys. Rev. B* **1988**, *37*, 785−789.
(58) (a) Dunning, T. H., Jr.; Hay, P. J. *Modern Theoretical Chemistry*; Schaefer, H. F., III, Ed.; Plenum: New York, 1976; Vol. 3, p 1. (b) Hay, P. J.; Wadt, W. R. *J. Chem. Phys.* **1985**, *82*, 270. (c) Wadt, W. R.; Hay, P. J. *J. Chem. Phys.* **1985**, *82*, 284−298. (d) Hay, P. J.; Wadt, W. R. *J. Chem. Phys.* **1985**, *82*, 299−310.
(59) (a) McClean, A. D.; Chandler, G. S. *J. Chem. Phys.* **1980**, *72*, 5639−5648. (b) Krishnan, R.; Binkley, J. S.; Seeger, R.; Pople, J. A. *J. Chem. Phys.* **1980**, *72*, 650−654. (c) Wachters, A. J. H. *J. Chem. Phys.* **1970**, *52*, 1033−1036. (d) Hay, P. J. *J. Chem. Phys.* **1977**, *66*, 4377−4384. (e) Raghavachari, K.; Trucks, G. W. *J. Chem. Phys.* **1989**, *91*, 1062−1065. (f) Binning, R. C.; Curtiss, L. A. *J. Comput. Chem.* **1995**, *103*, 6104. (g) McGrath, M. P.; Radom, L. *J. Chem. Phys.* **1991**, *94*, 511−516.
(60) Harvey, J. N. *Annu. Rep. Chem., Sect. C* **2006**, *102*, 203.
(61) Harvey, J. N. *Struct. Bonding* **2004**, *112*, 151−184.
(62) Harvey, J. N.; Aschi, M. *Faraday Discuss.* **2003**, *124*, 129−143.
(63) (a) Becke, A. D. *Phys. Rev. A* **1988**, *38*, 3098−3100. (b) Perdew, J. P. *Phys. Rev. B* **1986**, *33*, 8822−8824.

Tables of atomic coordinates for all the optimized species are available in the Supporting Information.

Results and Discussion

Synthesis of Complexes. The six iminopyrrole ligand precursors **1a–f** used in this work (Scheme 1) were prepared by condensation of 2-formylpyrrole or 2-acetylpyrrole with different arylamines (aniline, 2,6-dimethylaniline, and 2,6-diisopropylaniline), following the methods described in an earlier publication of our group.[33] The synthesis of formiminopyrrole derivatives is relatively straightforward, and standard conditions were employed.[33–37] However, the preparation of the new acetiminopyrrole derivatives required forcing conditions (no solvent and longer reflux) and resulted in lower yields. The yields in formimines vary from 60 to 70%, and those of acetimines are in the range 15–30%, decreasing with increasing R′ size. The crystal structure of the bulkier ligand precursor **1f** was determined (see below).

Deprotonation of the ligand precursors with NaH, in THF, followed by addition of the resulting solution to a THF suspension of anhydrous $CoCl_2$, in a molar ratio of 2:1 (ligand precursor:$CoCl_2$), gave rise to complexes **3a–f** (Scheme 2). The resulting unsaturated [Co(iminopyrrolyl)$_2$] complexes were extracted in hexane and precipitated by storage at −20 °C, yielding brown (**3a–c**), dark red (**3d,e**), and red (**3f**) powders or crystals, in good yields. All the syntheses have been carried out under rigorous inert atmosphere conditions since all compounds have shown to be very sensitive to air, especially when in solution. The synthesis of compound **3e** was already reported in the literature by Bochmann et al.,[13] but it was only characterized by elemental analysis and mass spectrometry. This preparation employed a slightly different procedure, using the corresponding Li salt of the ligand precursor and diethyl ether as solvent, leading however to a much lower yield (25%).

X-ray Diffraction. Crystals suitable for X-ray diffraction were obtained in the cases of compounds **1f** and **3e,f** enabling the determination of their crystal structures.

The molecular structure of the ligand precursor **1f** is shown in Figure 1. The asymmetric unit of the ligand precursor **1f** contains two independent molecules. Selected bond distances (Å) and angles (deg) are listed in the Figure 1 caption (for molecule 1). The pyrrole ring shows bond distances within 1.36–1.38 Å and a longer value of 1.408(2) Å for C2−C3. The coplanarity of the pyrrole ring with the acetimine group (torsion angle N2−C5−C4−N1 of 1.29°) and a distance C4−C5 of 1.456(2) Å, a value shorter than normal for a typical C−C single bond, points to an extension of the pyrrole ring π-electronic delocalization toward its acetimino substituent. The steric hindrance produced by the two isopropyl substituents, at the 2 and 6 positions of the phenyl ring, makes it nearly perpendicular (87.8°) to the acetiminopyrrole plane defined by atoms N2−C5−C4−N1. These features only change slightly upon coordination as it can be seen in Table 2 and are comparable to those observed for a similar compound with a mesityl substituent.[33]

The molecular structures of complexes **3e** (Figure 2) and **3f** (Figure 3) show tetrahedral and square-planar geometries

Scheme 2. Synthesis of Complexes **3a–f**

3f

2f

$CoCl_2$

2a-e

3a-e
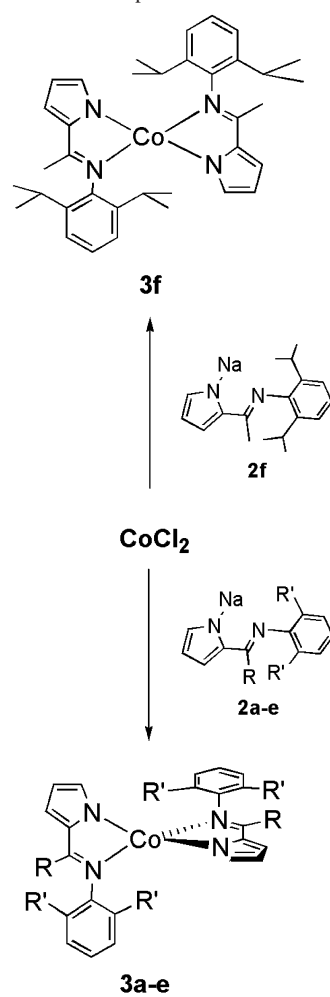
2a, 3a R = R′= H,
2b, 3b R = Me, R′= H
2c, 3c R = H, R′ = Me
2d, 3d R = R′ = Me
2e, 3e R = H, R′ = ^{i}Pr

around the Co center, respectively. Table 2 also lists selected bond distances and angles for **3e,f**.

The crystallographic structure of compound **3e** consists of an asymmetric unit containing two independent tetrahedral molecules. The planes defined by the five-membered rings Co1−N1−C4−C5−N2 and Co1−N3−C10−C11−N4 are more deviated from perpendicular (dihedral angles = 80.3−82.5°) than those reported in the literature (89.7°[3] and 85.1−86.2°[4]) for the two reported crystallographic structures of similar tetrahedral Co(II) iminopyrrolyl complexes. These compounds contain *tert*-butyl groups as substituents of the imine nitrogen, which are less sterically demanding than the 2,6-diisopropylphenyl groups used in the present work. The chelate bite angles N1−Co1−N2 and N3−Co1−N4 are respectively 82.5−83.0° (molecule 1) and 82.8−83.4° (molecule 2), while the angles N1−Co1−N3 and N2−Co1−N4 are 120.2−125.2 and 114.6−119.1°, showing a distorted tetrahedral geometry. The Co−N$_{pyrrolyl}$ bonds (1.952(8)−
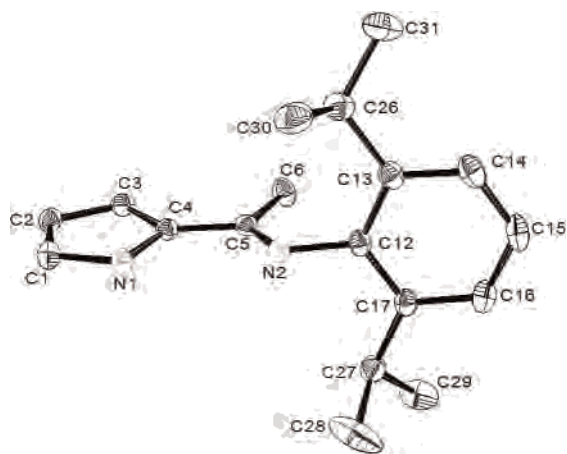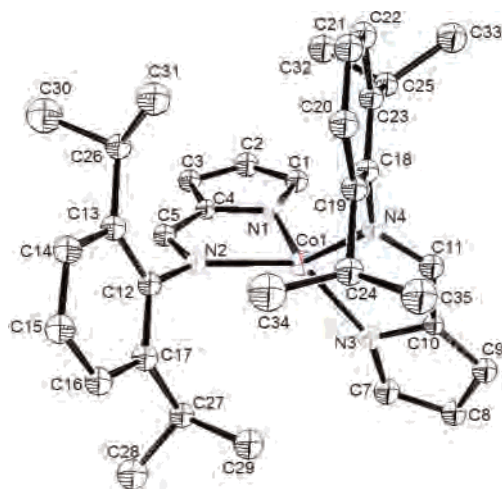
Figure 1. ORTEP III diagram of the ligand precursor **1f** (molecule 1 of the asymmetric unit) using 30% probability level ellipsoids. Hydrogens were omitted for clarity. Selected bond distances (Å) and angles (deg) for molecule 1: N1−C4 1.3729(19), N1−C1 1.3604(19), C1−C2 1.369(2), C2−C3 1.408(2), C3−C4 1.381(2), C4−C5 1.456(2), C5−C6 1.507(2), N2−C5 1.2835(19), N2−C12 1.4295(18); C5−N2−C12 120.03(12), C6−C5−N2 124.51(13), N2−C5−C4 118.88(13), C5−C4−N1 121.82(13), N1−C4−C3 107.25(13), C4−N1−C1 109.42(13), C2−C1−N1 108.51(14), C3−C2−C1 107.18(13), C4−C3−C2 107.64(14).

Table 2. Selected Bond Distances (Å) and Angles (deg) for Complexes **3e** and **3f**

	3e		
param	molecule 1	molecule 2	**3f**
Distances (Å)			
Co1−N1	1.985(9)	1.961(8)	1.9388(13)
Co1−N2	2.060(8)	2.054(8)	1.9528(14)
Co1−N3	1.971(8)	1.952(8)	
Co1−N4	2.055(8)	2.034(7)	
N1−C4	1.358(11)	1.383(12)	1.382(2)
N1−C1	1.369(12)	1.373(12)	1.356(2)
C1−C2	1.381(14)	1.385(13)	1.387(2)
C2−C3	1.364(13)	1.402(15)	1.394(3)
C3−C4	1.429(14)	1.384(13)	1.393(2)
N2−C5	1.332(12)	1.300(10)	1.307(2)
N2−C12	1.470(12)	1.455(12)	1.431(2)
N3−C7	1.360(12)	1.355(12)	
N3−C10	1.397(11)	1.377(11)	
N4−C11	1.297(11)	1.308(11)	
N4−C18	1.427(11)	1.447(12)	
C5−C6			1.492(2)
C4−C5	1.387(13)	1.416(13)	1.414(2)
C12−C13	1.401(13)	1.425(13)	1.415(2)
C13−C26	1.502(13)	1.487(13)	1.521(2)
Angles (deg)			
N1−Co1−N2	82.5(3)	83.0(3)	82.15(6)
Co1−N1−C4	110.1(7)	112.0(7)	112.21(11)
Co1−N1−C1	143.1(7)	143.4(7)	142.42(13)
C4−N1−C1	106.6(9)	104.4(8)	105.37(14)
Co1−N2−C5	109.9(7)	109.5(7)	115.31(11)
Co1−N2−C12	132.1(6)	130.2(6)	125.74(11)
C5−N2−C12	117.8(8)	120.3(8)	118.70(14)
C6−C5−N2			124.45(15)
C6−C5−C4			120.77(15)
N2−C5−C4	117.3(9)	120.2(10)	114.71(15)
C5−C4−N1	119.5(10)	115.2(9)	115.50(15)
C5−C4−C3	130.9(10)	132.6(10)	133.47(16)
N1−C4−C3	109.6(10)	112.2(10)	110.87(15)
C4−C3−C2	105.5(10)	105.0(10)	105.65(15)
C3−C2−C1	108.5(11)	107.5(10)	107.04(15)
C2−C1−N1	109.7(10)	110.8(10)	111.06(16)

1.985(9) Å) are shorter than the Co−N$_{imine}$ ones (2.034(7)−2.055(8) Å) due to the anionic nature of the pyrrolyl nitrogen and the steric bulk of the 2,6-diisopropyl substituents of the

Figure 2. ORTEP III diagram of complex **3e** (molecule 1 of the asymmetric unit) using 30% probability level ellipsoids. Hydrogens were omitted for clarity.
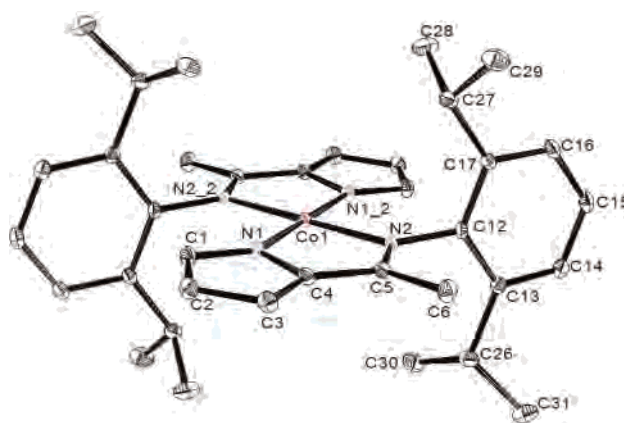
Figure 3. ORTEP III diagram of complex **3f** using 30% probability level ellipsoids. Hydrogens were omitted for clarity.

phenyl ring. These distances are very similar to those reported for a similar Co(*tert*-butylformiminopyrrolyl)$_2$ (1.981(7) and 2.066(8) Å, respectively).[3] The recently reported binuclear Co(II) complex containing two fragments of Co(*tert*-butyl-formiminopyrrolyl)$_2$,[4] bridged by a CMe$_2$ group bound to the pyrrolyl carbons adjacent to the N atoms, also shows similar distances (1.980(3)−1.989(3) and 2.047(3)−2.055-(3) Å, respectively). The angle between the planes defined by the two aryl rings of each molecule of the asymmetric unit of **3e** is 21.3 and 33.8°, respectively.

The crystallographic structure of compound **3f** shows an asymmetric unit formed by a half-molecule of [Co((2,6-diisopropylphenyl)acetiminopyrrolyl)$_2$] with the Co atom occupying a special position (0, 0, 0). The corresponding molecular structure is generated by symmetry, giving rise to a rare square planar geometry around the Co atom, which is located in an inversion center (Figure 3). Consequently, the Co atom is perfectly located in the plane formed by the four coordinating nitrogen atoms, meaning that the sum of angles around the Co atom is 360° (being N1−Co−N2 of 82.15(6)° and N1−Co−N2_2 of 97.85(6)°). The pyrrolyl rings, and thus the imine groups, lie trans to each other. The corresponding distances Co1−N1 (1.9390(14) Å) and Co1−N2 (1.9530(14) Å) are smaller than those found in the

Table 3. Effective Magnetic Moments μ_{eff} (μ_B) for Complexes **3a–f**, Measured in Toluene Solution (Evans Method) and in Powder (Dc Extraction Method), at 300 K

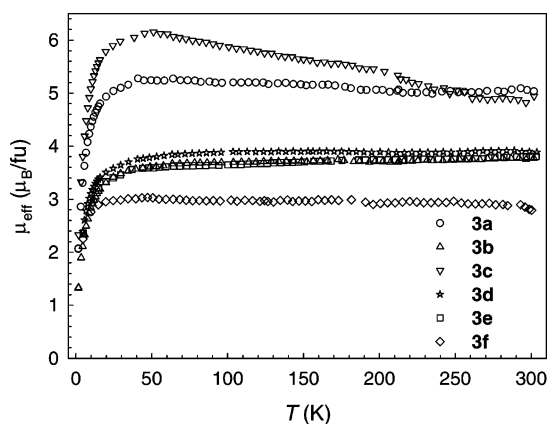| complex	Evans μ_{eff} (μ_B)	dc extractn μ_{eff} (μ_B)
3a	4.26	4.85
3b	4.29	3.77
3c	4.21	4.85
3d	4.24	3.90
3e	4.24	3.85
3f	2.40	2.85

tetrahedral complex **3e**, particularly that of the imine Co1–N2 distance that is significantly shorter (ca. 0.1 Å) than in **3e**. This may indicate a stronger σ-donor character of N2 atom in **3f** induced by the methyl (C6) substituent of the iminic carbon (C5), which may also cause a higher degree of steric congestion around the Co atom (see below, in Molecular Orbital calculations). In fact, the 2,6-diisopropyl-phenyl groups are nearly perpendicular to the CoN$_4$ square plane (82.3°) and parallel to each other (0°). Interestingly, an edge-to-face interaction between C1–H and the aryl centroid of **3f** (C1–H···aryl centroid = 2.376 Å) seems to take place, although it may be a consequence of this congestion. These features prevent the most favorable tetrahedral arrangement to take place, forcing a different low-spin ($S = 1/2$) electronic configuration of the Co atom. Usually, Co(II) tetracoordinated with nitrogen-donor chelating ligands show a clear preference for high-spin tetrahedral geometry ($S = 3/2$).

For both **3e,f**, the imine double bond C5–N2 distances (1.312(10)–1.306(2) Å) are longer than that of the free ligand (namely 1.283(2) Å for **1f**), showing some degree of π–π^* back-bonding from the metal to the imine fragment.

Magnetic Measurements. The results obtained for the magnetic susceptibility measurements of the different complexes, taken both in solution (Evans method) and in powder (dc extraction method), are shown in Table 3.

In solution measurements, at 300 K, the values of μ_{eff} found for complexes **3a–e** are very similar (ca. 4.2–4.3 μ_B) and lie in the range typical of known tetrahedral Co(II) complexes (4.2–5.1 μ_B) with $S = 3/2$.[4,27,28,32,64] These values are higher than the expected spin-only value of 3.87 μ_B, suggesting the presence of spin–orbit coupling effects.[4,32,64] On the other hand, complex **3f** is the only one in the series which μ_{eff} value (2.4 μ_B) fall within the typical range of low-spin $S = 1/2$ square-planar Co(II) complexes (2.0–2.7 μ_B),[28,32,64,65] although values such as 1.75 μ_B were also reported in the literature,[26] which are very similar to the calculated $S = 1/2$ spin-only value of 1.73 μ_B. The μ_{eff} value obtained for complex **3f**, containing the bulkiest iminopyr-rolyl in the ligand series, shows also significant spin–orbit coupling effects but points clearly to a square-planar structure, which was also confirmed by X-ray diffraction (see above).

Figure 4 shows the temperature dependence of the effective magnetic moment ($\mu_{eff} = 2.83(\chi T)^{1/2}$ μ_B) obtained for

(64) Cotton, F. A.; Wilkinson, G. *Advanced Inorganic Chemistry*, 5th ed.; John Wiley and Sons: New York, 1988.
(65) Greenwood, N. N.; Earnshaw, A. *Chemistry of the Elements*; Pergamon Press: London, 1984.

Figure 4. Temperature dependence of the effective magnetic moment, μ_{eff}, of the complexes **3a–f**, in the range 5–300 K (dc extraction method).

polycrystalline powder samples of complexes **3a–f**, using the dc extraction method.

In general, the values are similar and show the same trend observed for the magnetic moments determined in toluene solution, although values obtained for complexes **3a,c** (formimino derivatives) are slightly higher and those of complexes **3b,d,e** are somewhat lower, the latter lying close to the spin-only value. The slight increase of the magnetic moments of **3a,c**, as temperature decreases to 50 K, also reinforces the presence of significant spin–orbit coupling effects. Below 10 K the decrease in μ_{eff} suggests the presence of very weak intermolecular magnetic interactions. At the lower temperature, 1.7 K, the values of the magnetic field dependence of the magnetization, $M(B)$ (see Supporting Information), show some tendency to saturate at higher fields, and the linearity of the $M(B)$ curves obtained for higher temperatures confirms their paramagnetic behavior.

For all the complexes, cooling–warming cycles of magnetization versus temperature, in the temperature range 300–5 K, give exactly the same values. This behavior indicates that no spin-crossover equilibria occur between $S = 3/2$ and $S = 1/2$ ground states, which may be associated with a high-energy barrier of the tetrahedral to square planar interconversion.

Electronic Spectra. The spectra of the ligand precursors **1a–f** and of complexes **3a–f** were recorded in the range 200–1500 nm, in toluene solutions, under nitrogen atmosphere. Their comparison enabled assignment of all bands observed in the range 270–350 nm to intraligand (IL) transitions. The toluene cutoff prevented the spectra visualization below 270 nm, being that the spectra of the ligand precursors were also recorded in Nujol mulls. According to the literature,[32,66] the bands observed above 400 nm may be assigned to transitions involving Co(II) ions. Table 4 summarizes the results obtained for the complexes studied above 400 nm. All the compounds **3a–f** show bands in the range 450–640 nm. On the basis of their molar extinction coefficients ($10 < \epsilon < 850$ L mol^{-1} cm^{-1}), these electronic absorptions can be assigned to d–d transitions.[32,66] In particular, for the square-planar complex **3f**, it can also be

(66) Lever, A. B. P. *Inorganic Electronic Spectroscopy*; Elsevier: Amsterdam, 1968.

Table 4. Absorption Maxima Values (nm) and, in Parentheses, Molar Extinction Coefficients (L mol^{-1} cm^{-1}) Taken from the Electronic Spectra (above 400 nm) of Complexes **3a**–**f** in Toluene at Room Temperature[a]

3a	3b	3c	3d	3e	3f	obsd[b]
410 (sh, 1500)	410 (sh, 850)	410 (sh, 7500)	400 (sh, 16 400)	410 (sh, 600)		CT or dd
440 (sh, 270)	435 (sh, 490)					dd
		490 (sh, 247)	490 (sh, 124)	484 (sh, 549)	460 (sh, 1000)	dd
		535 (sh, 225)	535 (sh, 113)	523 (sh, 462)	544 (sh, 500)	dd
635 (sh, 35)	640 (sh, 54)	630 (sh, 33)	630 (sh, 17)	631 (sh, 39)		dd
					1152 (8)	dd

[a] sh = shoulder. [b] Tentative band assignment: CT = charge transfer; d–d = metal d orbital internal transitions.

**Chart 2** Four Structures Optimized by DFT (R = H or Me)

square planar
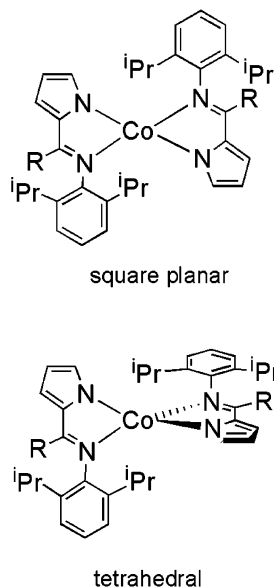
tetrahedral

seen an extra band in the near-infrared region (1152 nm), which is predicted in the literature.[66] A corresponding band is not present in the spectra of the tetrahedral **3a**–**e** complexes. Such a difference between the electronic spectra of square-planar and tetrahedral d^7 Co(II) complexes was also noticed by Lippard et al.[32]

Molecular Orbital Calculations. The structural characterization of the complexes clearly shows **3a**–**e** as tetrahedral species whereas **3f** is square planar. To better understand this structural preference, DFT calculations[54] were performed on complexes **3e,f**, which are those containing the bulkier ortho aryl substituents (^{i}Pr) and the only ones with available X-ray structures. Their chemical difference lies only in the iminic carbon substituent of the iminopyrrolyl ligand, R = H (**3e**) or Me (**3f**) (see Chart 2). Thus, for each R group (H or Me), two coordination geometries were tested, square planar and tetrahedral, representing a total of four different species.

The optimized geometries of the complexes with R = H (complex **3e**) in the two coordination geometries are shown in Figure 5. The square planar molecule (top of Figure 5) presents a practically undistorted geometry, close to an ideal square planar structure. The angle between the planes of the two five-membered rings CoNCCN is 0°, and the 2,6-diisopropylphenyl groups are perpendicular to the corresponding five-membered ring, the angle between the plane of the aryl ring and the five-membered ring being 90°. The

four Co–N distances are well within bonding values (1.95 and 1.98 Å).

The geometry calculated for the tetrahedral species with R = H (bottom of Figure 5) compares fairly well with the corresponding X-ray structure (Figure 2). For example, the calculated Co–N bonding distances are in the range 2.01–2.09 Å, being close to the experimental values: 1.95–2.06 Å (there are two molecules in the asymmetric unit, in the corresponding X-ray crystal structure). A reasonable agreement is also observed for the relevant angles. The angle between five-membered rings is 79° (calcd) compared with 80–83° (expt), revealing a somewhat distorted structure with respect to an ideal tetrahedral where the corresponding angle would be 90°. The orientation of the 2,6-diisopropylphenyl groups with respect to the five-membered rings is not perpendicular as in the square planar molecule, being instead tilted: the angles between the aryl ring and the five-membered ring are 67° (calcd) and 58–75° (expt) (as there are two molecules in the asymmetric unit, in the corresponding X-ray crystal structure). The reason for this distortion, that is, the deviation of those angles from 90°, is evident in the optimized geometries represented in Figure 5. In fact, a tetrahedral coordination forces the proximity of the 2,6-diisopropylphenyl substituents of the two different N–N
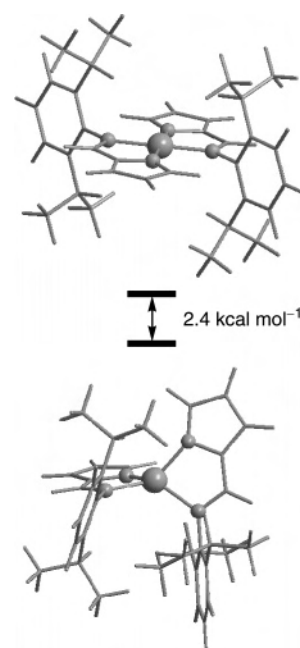
Figure 5. Optimized geometries (B3LYP) for complex **3e** (with R = H) with square planar (top) and tetrahedral (bottom) geometries. The Co and the coordinating N atoms are highlighted, and the energy difference (kcal mol^{-1}) between the two species is presented.
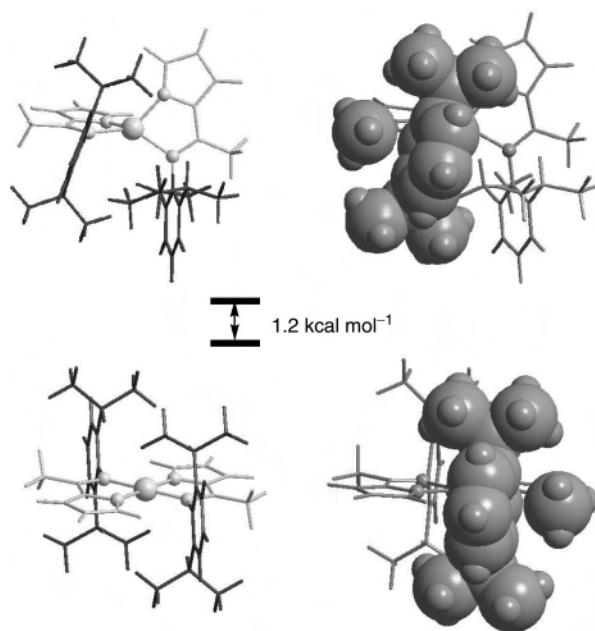
Figure 6. Optimized geometries (B3LYP) for complex **3f** (with R = Me) with square planar (bottom) and tetrahedral (top) geometries. The Co and the coordinating N atoms are highlighted, and the energy difference (kcal mol^{-1}) between the two species is presented. On the left-hand side, the structures are represented with the 2,6-diisopropylphenyl groups in dark gray. On the right-hand side, for each molecule, one 2,6-diisopropylphenyl and the methyl in the adjacent carbon atom are presented with space-filling representations.

ligands, while in the square planar environment those substituents lie in opposite sides of the molecule, in a trans geometry. As a consequence, a tilting from perpendicularity of both the angle between the two CoNCCN five-membered rings and the angle between the phenyl ring and the respective five-membered ring is required to keep the substituents away from each other, specially the bulky isopropyl groups. Despite this geometrical distortion, the tetrahedral isomer is calculated to be the most stable (by 2.4 kcal mol^{-1}). Thus, the high electron pairing energy characteristic of first row transition metals such as Co(II) (d^7) favors the high-spin molecule (tetrahedral, $S = 3/2$) with respect to the low-spin species (square planar, $S = 1/2$).

The optimized geometries for the complexes with R = Me (complex **3f**) are represented in Figure 6. The structure calculated for the square planar molecule (bottom of Figure 6) compares well with the experimental one, obtained by X-ray diffraction (Figure 3), both in what concerns the Co−N bonding distances (calcd, 1.95−2.00 Å; expt, 1.94−1.95 Å) as in the relevant angles. The two five-membered rings are coplanar since the angle between CoNCCN planes is 0° in the calculated and in the experimental structures. The aryl rings are essentially perpendicular to the corresponding five-membered ring with angles close to 90° between the C$_6$ and the CoNCCN planes (calcd, 88°; expt, 82°).

The structure calculated for the tetrahedral complex (R = Me, top of Figure 6) is similar to the one optimized for the species with R = H in its main geometrical features. The four Co−N distances are well within bonding values (2.00−2.09 Å), the angle between CoNCCN planes (80°) deviates from 90°, and the 2,6-diisopropylphenyl groups are tilted

with respect to the five-membered ring planes (73°). However, the relative stability between the two coordination geometries is reversed. In the case of the complexes with R = Me the square planar molecule is favored by 1.2 kcal mol^{-1} with respect to the tetrahedral complex. A stereochemical reason can be partially responsible for this change as highlighted by the space-filling representations of Figure 6. In fact, the presence of the methyl substituents in the carbon adjacent to the nitrogen atom of the ligand restrains the tilting of the 2,6-diisopropylphenyl groups as shown by the corresponding angles: 67 and 73°, for R = H and Me, respectively. As a consequence of the repulsion between methyl and 2,6-diisopropylphenyl, this substituent is pushed closer to the corresponding group in the opposite iminopyrrolyl ligand, originating a more crowded environment around the metal and causing some destabilization in the molecule. For example, the closest C−C contact between isopropyl groups in different iminopyrrolyl ligands is 4.34 Å in the tetrahedral complex with R= H (**3e**) and becomes 4.08 Å in the equivalent molecule with R = Me (**3f**).

In addition, electronic factors can also favor the square planar geometry in **3f**. Comparing the two square planar complexes, the HOMO−LUMO gap calculated for the complex with acetiminopyrrolyl (R = Me) is 0.1 eV higher than that obtained for the complex with formiminopyrrolyl (R = H), indicating the former is a higher field ligand and, thus, expected to favor the low-spin complex.

Conclusions

A new series of Co(II) complexes **3a**−**f** [Co($\kappa^2 N, N'$-NC$_4$H$_3$C(R)=N-2,6-R$'_2$C$_6$H$_3$)$_2$] (R = R' = H, **3a**; R = Me, R' = H, **3b**; R = H, R' = Me, **3c**; R = R' = Me, **3d**; R = H, R' = ^{i}Pr, **3e**; R = Me, R' = ^{i}Pr, **3f**) was prepared. The complexes contain bidentate iminopyrrolyl ligands with increasing bulkiness. Magnetic susceptibility measurements, in powder and in solution, X-ray diffraction, and UV/vis/NIR proved that complexes **3a**−**e** exhibit tetrahedral geometry, whereas complex **3f** showed a rare square planar geometry. DFT calculations suggest that the preference of a square planar geometry, in the case of complex **3f**, probably results from a combination of stereochemical interligand repulsion and electronic factors. On one hand, a square planar geometry allows larger separations between the substituents (R and R') of the iminopyrrolyl ligands, and on the other, the iminopyrrolyl ligand with R = Me is a stronger donor, favoring the low-spin molecule.

Supporting Information Available: CIF files containing X-ray structural data, including data collection parameters, positional and thermal parameters, and bond distances and angles, for complexes

1f and **3e**,**f**, figures containing the magnetic field dependence of the magnetization, $M(B)$, for all complexes, at 1.7 and 25 K, a table containing the absorption maxima of the electronic spectra UV region of complexes **3a**−**f**, and a table of atomic coordinates for the optimized species (**3e**,**f**) obtained with B3LYP/B1. This material is available free of charge via the Internet at http://pubs.acs.org.